Materials Research Letters

ISSN: (Print) 2166-3831 (Online) Journal homepage: http://www.tandfonline.com/loi/tmrl20

Nanoporous Gold—Testing Macro-scale Samples to Probe Small-scale Mechanical Behavior

Nadiia Mameka, Ke Wang, Jürgen Markmann, Erica T. Lilleodden & Jörg Weissmüller

To cite this article: Nadiia Mameka, Ke Wang, Jürgen Markmann, Erica T. Lilleodden & Jörg Weissmüller (2016) Nanoporous Gold—Testing Macro-scale Samples to Probe Small-scale Mechanical Behavior, Materials Research Letters, 4:1, 27-36, DOI: 10.1080/21663831.2015.1094679

To link to this article: https://doi.org/10.1080/21663831.2015.1094679

Published online: 16 Oct 2015.

MATERIALS RESEARCH LETTERS

Mater. Res. Lett., 2016
Vol. 4, No. 1, 27–36, http://dx.doi.org/10.1080/21663831.2015.1094679

Taylor & Francis
Taylor & Francis Group

www.tandfonline.com/toc/tmrl20/current

Nanoporous Gold—Testing Macro-scale Samples to Probe Small-scale Mechanical Behavior

Nadiia Mameka[a], Ke Wang[b], Jürgen Markmann[a,b], Erica T. Lilleodden[a] and Jörg Weissmüller[a,b]*

[a]*Helmholtz-Zentrum Geesthacht, Institut für Werkstoffforschung, Werkstoffmechanik, Geesthacht, Germany*
[b]*Technische Universität Hamburg-Harburg, Institut für Werkstoffphysik und -technologie, Hamburg, Germany*

(*Received 30 July 2015; final form 11 September 2015*)

Nanoporous gold made by dealloying exemplifies how the exciting mechanical properties of nanoscale objects can be exploited in designing materials from which macroscopic things can be formed. The homogeneous microstructure and the possibility of adjusting the ligament size, L, between few and few hundred nm, along with the high deformability and reproducible mechanical behavior predestine the material for model studies of small-scale plasticity using reliable macroscopic testing schemes on mm- or cm-size samples. Such experiments tend to agree with the Gibson-Ashby scaling relation for strength versus solid fraction, while suggesting an essentially L^{-1} scaling of the local strength of the ligaments. By contrast, the elastic compliance is dramatically enhanced compared to the Gibson-Ashby relation for the stiffness. Contrary to intuition, the anomalously compliant behavior of the nanomaterial goes along with a trend for more stiffness at smaller L. This article discusses surface excess elasticity, nonlinear elastic behavior and specifically shear instability of the bulk, network connectivity, and the surface chemistry as relevant issues which deserve further study.

Keywords: Nanoporous Gold, Dealloying, Scaling Relations, Surface Excess Elasticity, Connectivity, Hybrid Materials

1. Introduction The use of small-scale heterogeneity as a means of strengthening is ubiquitous in materials science. Dispersion strengthening is the most obvious example, and the simplest, lightest, and most affordable strengthening dispersoid is a pore.[1] Thus, introducing a small amount of porosity can make a material stronger by taking part of it away. Nanoporous metals explore a different region of parameter space, in which the pores are the majority component and the solid takes to form of a network of nanoscale struts (or 'ligaments'). Their small scale is important, since the trend of smaller is stronger implies a partial compensation of the loss in strength that comes with removing most of the solid. Nanoporous metals, and specifically those made by dealloying, thus provide a materials base for exploring the simultaneous impact of porosity and of nanoscale structuring on mechanical behavior.[2–5]

As the most extensively studied dealloying-made material, nanoporous gold (NPG) exhibits a perfectly conventional polycrystalline microstructure with tens or hundreds of micron grain size. The highly ordered crystal lattice of each grain is porous, and the prevalent microstructural feature is the uniformly interconnected network of nanoscale ligaments that contain the occupied lattice sites.[6,7] When alloyed with Pt, samples of NPG can be made with characteristic mean ligament diameters, L, down to the unusually small scale of 5 nm,[8,9] and thermal coarsening results in self-similar growth to L close to 1 μm.[10,11] This affords studies of size-dependence with L spanning more than two orders of magnitude in size, a dynamic range that is not typically accessible with other types of nanomaterial and that provides for particularly significant experimental data on size-effects.

After initial studies of NPG used small-scale testing schemes,[2,12–18] it is now possible to make cm-size samples that can be subjected conventional macroscopic compression [7,11,19–22] or even tension [11,23,24] tests. The large strain that is reached in compression affords testing protocols comprising, for example, strain-rate jumps [7] or load-unload segments.[25] Besides enabling model studies of small-scale mechanical behavior, macroscopic NPG samples also demonstrate the implementation of the favorable mechanical behavior that is suggested by academic studies of nanoscale objects (nanowires, nanopillars) into a 'material', that is,

*Corresponding author. Email: weissmueller@tuhh.de

into a substance from which things—such as engineering components—can be formed.

NPG exhibits an unusually large specific surface area, emphasizing the impact of surface phenomena on the materials effective macroscopic mechanical response. As a by-product of the synthesis by alloy corrosion (typically) under potential control in electrolyte, electrochemical characterization affords a precise knowledge and control of the surface alloy chemistry and adsorbate coverage, providing unprecedented information on the surface state.[26–28]

Here, we discuss selected current issues in small-scale plasticity and elasticity emerging from studies using macroscopic tests and NPG as the model material.

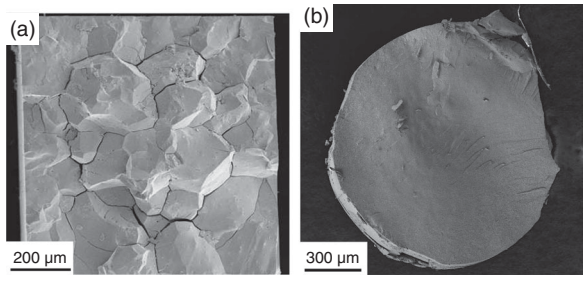

Figure 2. Cleavage surfaces of NPG samples prepared by dealloying (a) $Au_{25}Cu_{75}$ (from [31]) and (b) $Au_{25}Ag_{75}$. Note intergranular cracking in (a) versus intragranular cracking in (b).

2. Microstructure The elementary processes of nanoporosity formation by dealloying are simply the dissolution of the less noble element and the reorganization of the more noble element between different lattice sites by surface diffusion.[29,30] In the consequence, (i) the nanoscale pore structure represents a new length-scale that is formed during corrosion and that has no equivalent in the original, uniform solid solution of the master alloy, and (ii) no new crystals are nucleated, so that the emerging nanoporous structure decorates the original crystal lattice. The transmission electron micrograph of Figure 1(a) illustrates interconnected ligaments, ~ 50 nm in size, in a cross-section through NPG,[11] while the electron backscatter diffraction (EBSD) image, Figure 1(b), of the crystallographic orientation of a sample prepared under similar conditions shows a perfectly ordered polycrystalline microstructure with a mean grain size of tens μm,[7] three orders of magnitude larger than the pore- or ligament size of the same sample.

Besides crystallography and ligament size, the defect structure that may be created during dealloying is crucial for the mechanical performance of macroscale nanoporous samples. The corrosion rate controls volume shrinkage [6] and, thereby, the formation of native cracks which impair the deformability. Slow corrosion [6] and the use of slightly elevated temperature [7] helps to mitigate this problem. The corrosion behavior of grain boundaries is equally relevant, as illustrated in Figure 2. NPG samples are readily cleaved by applying slight pressure with a scalpel, and Figure 2(a) shows the resulting cleavage surface of a sample made by dealloying carefully annealed $Cu_{75}Au_{25}$. The intergranular nature of the fracture is apparent, as are crack branches that propagate along grain boundaries. The observation has been linked to preferential attack of Cu-rich boundaries due to Cu grain boundary segregation in the master alloy during the homogenization anneal.[31] In fact, suppressing the homogenization anneal in Cu-Au removes the problem,[31] as does replacing Cu-Au with Ag-Au as the master alloy. Figure 2(b) illustrates the intragranular fracture that is characteristic of NPG samples—here made from $Ag_{75}Au_{25}$—with high deformability.

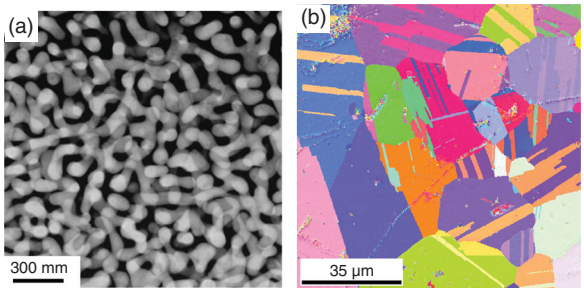

Figure 1. Microstructure of NPG on different length scales. (a) Transmission electron microscopy shows the pore- and ligament structure, here for mean ligament size 50 nm (from [11]). (b) Electron backscatter diffraction (EBSD) map reveals ordered crystallites with grain size $> 10\,\mu$m, much larger than the ligament size (from [7]). Images are obtained from separate samples prepared under identical conditions.

3. Stress-strain behavior of NPG—empirical findings Several studies have investigated the dependency of the yield and flow behavior [2,7,11,13,16,21,23] as well as the stiffness [32,33] of NPG on L. Compression tests on highly deformable macroscopic samples are particularly meaningful, since they also afford an inspection of the variation of plastic and elastic properties as the microstructure changes during compression. Figure 3 illustrates this for a set of NPG samples with $L = 20, 40, 150$ nm.

The NPG specimens of this work, 2×1 mm in size as in Figure 3(a), were prepared according to the synthesis and coarsening protocols of [19]. As the only notable exception, the $Ag_{75}Au_{25}$ master alloy bodies were not cut from ingots but shaped by wire drawing and subsequent cutting with a diamond wire saw. After the electrochemical dealloying, repeated electrochemical oxidation-reduction cycles induced a minor coarsening,

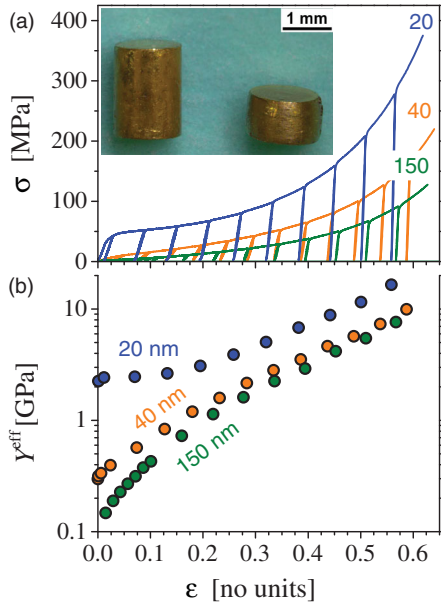

Figure 3. Compression behavior of NPG with mean ligament diameters $L = 20,\ 40,\ 150$ nm: (a) Graphs of stress, σ versus engineering compression strain, ε, including unload-reload cycles. Strain rate 10^{-4}s^{-1}. Insert: photographs of samples before and after compression. (b) Effective Youngs modulus, Y^{eff}, determined as secant modulus in the unload/reload segments, versus ε.

thereby diminishing the residual Ag to content to $\lesssim 5$ at.-%. The cycles, along with a final washing in ultrapure water, also served to ensure a clean, adsorbate-free surface. The solid volume fractions (as determined from macroscopic sample dimensions, mass, and composition) for samples with $L = 20, 40$, and 150 nm were $\varphi = 0.27 \pm 0.01$, 0.29 ± 0.02 and 0.32 ± 0.03, respectively. Mechanical tests used the procedures of [34].

In the compression tests of Figure 3(a), the enhanced flow stress at smaller L is apparent, as are the pronounced strain hardening and the quasi immediate onset of yielding, at extremely small load. Photographs of samples before and after deformation (inset in Figure 3) illustrate the deformability. Note also the small transverse plastic strain, implying that the compressive deformation is almost completely carried by densification of the nanoscale metal network. The deformation protocol in Figure 3(a) comprises unload-reload segments for monitoring the evolution of stiffness, as measured by the secant modulus, during deformation. The results, Figure 3(b), show that smaller L brings not only higher strength but also higher stiffness.

In our lab we have obtained data as in Figure 3 for several batches of samples made independently by several scientists. The above trends emerge as perfectly reproducible. We now discuss these findings in relation to the literature, highlighting remarkable aspects and open issues.

4. Scaling laws As a background for discussing the empirical findings on the mechanical behavior of NPG, it is useful to inspect scaling laws for stiffness and for strength of porous solids as the function of L and of the solid fraction, φ.

The impact of φ on the effective macroscopic values of Youngs modulus, Y^{eff}, and of strength, σ^{eff}, of certain porous materials is described by the Gibson-Ashby scaling laws.[35] Being set up for low-density cellular solids, these laws do not automatically apply to NPG. First, NPG samples in almost all reports (including the present study) have φ between 0.25 and 0.35, outside the range explored by Gibson and Ashby. Second, the network structure of NPG is ill compatible with the cellular architecture of foams. Yet, studies of the mechanical behavior of NPG more often than not use the Gibson-Ashby laws to obtain benchmarks to which the actual findings can be compared. Several of these studies even either report or even presuppose agreement,[2,5,7,12,13,16] while others discuss corrections.[22,23,36,37] Thus, even though it is now widely realized that the Gibson-Ashby scaling relations are not designed for network structures such as NPG, these relations remain indispensable as a starting point for discussing scaling in that material.

One of the Gibson-Ashby laws relates the effective macroscopic Young's modulus, Y^{eff}, to the local modulus, Y^{loc}, via [35]

$$Y^{\text{eff}} = Y^{\text{loc}}\varphi^2. \tag{1}$$

It is generally admitted (see e.g. [5]) that the apparent *local* stiffness at the ligament scale may depend on L. Mameka et al.,[34] considering the bending stiffness as the relevant parameter for the elastic response at the ligament level, present a simple argument for the impact of surface excess elasticity on the apparent Y^{loc}. The dependence of the surface stress on tangential strain defines a surface excess elastic constant, and an intuitively accessible parameterization of this constant is via an apparent excess of material at the surface, in other words an apparent thickening of the ligaments by the radius increment τ. The sign of τ decides whether the surface is stiffer ($\tau > 0$) or more compliant ($\tau < 0$) than bulk. In this approximate description, the size affects the apparent local stiffness via [34]

$$Y^{\text{loc}}_{\text{app}} = Y^{\text{loc}}\left(1 + \frac{8}{L}\tau\right). \tag{2}$$

In relation to strength, the Gibson-Ashby scaling for the effective macroscopic yield strength, $\sigma_{\text{y}}^{\text{eff}}$, of open-cell foams, applicable in the limit of small φ, states that [35]

$$\sigma_{\text{y}}^{\text{eff}} = 0.3\sigma_{\text{y}}^{\text{loc}}\varphi^{3/2}, \tag{3}$$

where $\sigma_{\text{y}}^{\text{loc}}$ is the local yield strength, in the present context the strength of individual ligaments. In terms of

characteristic constants L_0 and σ_0, experiment suggests that (for not too large L)

$$\sigma_{\rm y}^{\rm loc} = \sigma_{\rm y}^{0}\left(\frac{L}{L_0}\right)^{m}, \qquad (4)$$

and compression and tension tests on small-scale pillars of fcc metals find $m = -0.5$ to -1.0.[38] For NPG, results obtained with several small-scale testing schemes suggest $m \approx -0.6$,[5] yet tests on macroscopic samples [7] indicate the stronger size dependence $m \approx -1$ (see also below).

The Gibson-Ashby scaling relations implicitly require that the pore space is empty and so carries no load. Yet, it is also of interest to investigate the load-carrying ability of the metal phase when NPG, as the reinforcing phase, is embedded in polymer. Wang et al. [11] derive a rule of mixture for such interpenetrating-phase nanocomposites,

$$\sigma_{\rm y}^{\rm eff} = \sigma_{\rm y}^{\rm polymer}(1-\varphi) + \sigma_{\rm y}^{\rm loc}\varphi, \qquad (5)$$

where φ—quite analogously to its usage above—represents the metal volume fraction. The load carried by the metal phase (second term on the right-hand side of Equation (5)) here scales *linearly* with φ, quite contrary to the $\sigma_{\rm y}^{\rm eff} \propto \varphi^{3/2}$ scaling of the pure nanoporous metal. The smaller exponent in the composite is beneficial, since it implies that even small amounts of metal reinforcement are efficient in strengthening the composite.

5. Size-dependent strength In view of the early yield onset in compressive stress-strain curves of NPG such as Figure 3(a), the flow stress at 1% plastic strain has been used for parameterizing strength,[7] and Figure 4(a) shows how that parameter depends on the ligament size. The data is for samples from different batches of this work, along with results of macroscopic compression and microhardness tests in [7]. The high consistency of these results advertises NPG as an outstanding model system for studies of nanoscale mechanical behavior.

Figure 4(b) shows the L-dependence of the local strength $\sigma_{\rm y}^{\rm loc}$, as obtained by combining the data in Figure 4(a) with the scaling law Equation (3). The straight line of best fit in Figure 4(a) has slope -1.09 ± 0.08, supporting the observation, in [7], of a size-exponent near -1. Also presented is a compilation, originally due to Biener et al. [4] and extended by Jin et al.,[7] of results from small-scale tests on gold micro- and nano-objects and from nanoindendation of NPG. The trend of smaller is stronger is consistent for all data in the figure, yet the macroscopic samples are systematically weaker by a factor of three to four. The discrepancy remains—though at a lesser level—when the

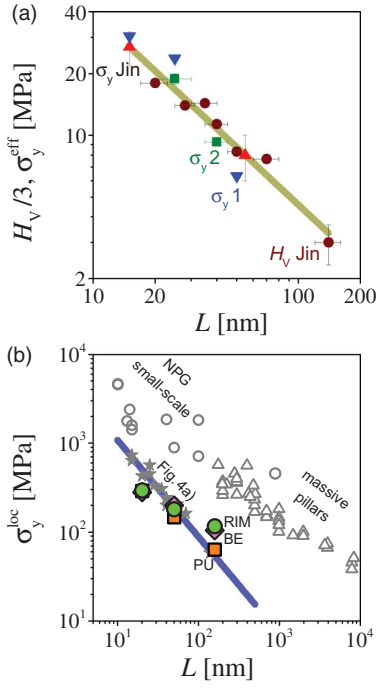

Figure 4. Size- (L-) dependent strength. (a) Effective macroscopic strength $\sigma_y^{\rm eff}$ from compression tests on bulk NPG samples. Symbols: averages over tests with several samples from any of two batches (labelled $\sigma_{\rm y}1, \sigma_{\rm y}2$) of this work, error bars: standard deviation over several samples. Data for $\sigma_y^{\rm eff}$ (from compression tests) or for converted Vickers hardness ($H_{\rm V}$) from Jin et al.,[7] is labelled 'Jin'. Straight line of best fit is shown to emphasize trend. (b) Local strength, $\sigma_y^{\rm loc}$, versus L. Line and grey stars: data and trend for mm-scale NPG samples, as inferred from part (a), using Equation (3). Straight line of best fit to that data (blue line) has slope -1.09 ± 0.08. Colored symbols: different NPG-based composites (as distinguished by labels RIM, BE, PU, see Figure 5), using Equation (5) with $\sigma_y^{\rm eff}$ data (from [11]). Results from small-scale tests on gold pillars (open triangles) and NPG (open circles) as compiled in [4,7] are shown for comparison.

nanoindentation-based data, which involves the assumption of Tabor factor 1 as applicable to macroscopic metal foams, are corrected to Tabor factor 3 as suggested by the experiments in [7].[1] Note also the difference in the size exponents.

Inconsistencies in the estimates for $\sigma_{\rm y}^{\rm loc}$ in NPG may, in principle, reflect an inadequate choice of scaling relations. It is therefore of interest that the scaling for interpenetrating phase-composites, Equation (5), provides an independent path to measuring the local strength, which does not rely on the Gibson-Ashby laws. Stress-strain curves by Wang et al. [11] for NPG-based composites are shown in Figure 5, and the colored symbols in Figure 4(b) represent the corresponding estimates of $\sigma_{\rm y}^{\rm loc}$. In view of the independent database and theory (data for pure NPG and Equation (3) versus data for composites and Equation (5)), the good agreement between the results for $\sigma_{\rm y}^{\rm loc}$ supports the applicability of

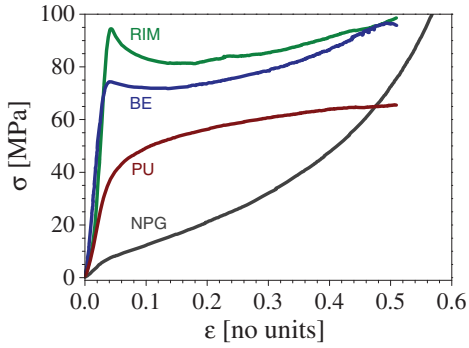

Figure 5. Compressive stress-strain graphs (strain rate 10^{-4} s^{-1}) of interpenetrating-phase nanocomposites made from NPG impregnated with bisphenol A ('RIM'), bisphenol F ('BE'), and polyurethane ('PU') resins. Result for pure NPG is shown for comparison. All samples have $L = 50$ nm. Data from [11].

the Gibson-Ashby law for the macroscopic NPG samples that are in the focus of the present work.

The different approaches to analyzing the strength of macroscopic NPG samples in terms of the scaling laws of Section 4 are supported by the consistency between their results. The discrepancy between the present results and literature data, as compiled in Figure 4(b), thus points toward a difference at the materials level. Findings for the stiffness underline that point.

6. Size-dependent stiffness Figure 6 examines the stiffness of NPG. Part (a) shows secant moduli from the load-unload segments of Figure 3(b), plotting the effective Young's modulus, normalized to Young's modulus of massive gold, versus the solid fraction φ as it varies during plastic compression. The Gibson-Ashby scaling, Equation (1), is shown for comparison. While the trend for stiffening during compression is expected as a consequence of the densification, the experimental stiffness values are not well described by the Gibson-Ashby scaling. This is exemplified by NPG with $L =$ 150 nm which, at the beginning of compression, exhibits $Y^{\text{eff}} = 148$ MPa, nearly 70-fold less than predicted by Equation (1). The low modulus is consistent with the high resilience of wet NPG as reported in [39].

Independent confirmation comes from molecular dynamics simulation [25] that uses an embedded-atom potential for gold. Studying NPG with 3.2 nm ligament size, the simulation finds the graph of $Y^{\text{eff}}(\varphi)$ and specifically the absolute value at low strain to practically coincide with that of the 40 nm sample in the experiments of Figure 3(a).

Based on finite element simulations, Huber et al. [22] have pointed out that structural disorder in nanoscale networks may substantially diminish the stiffness. Yet, their model does not reproduce the extremely high compliance and the fast stiffening during the initial

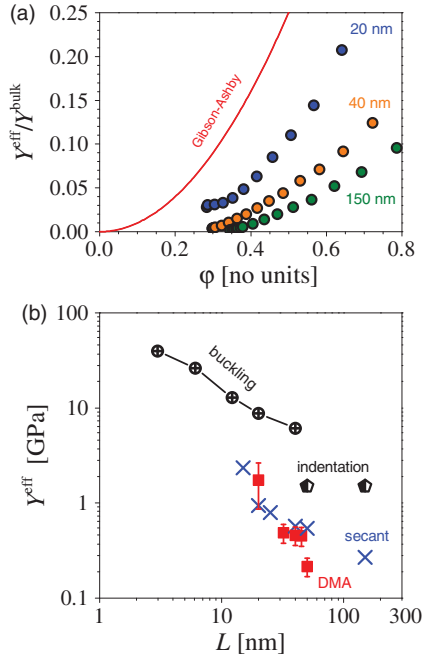

Figure 6. Effect of solid volume fraction φ and ligament size L on the effective elastic response of NPG in compression. (a) Normalized effective Young's modulus $Y^{\text{eff}}/Y^{\text{bulk}}$ versus φ for different L (labels; data from Figure 3) and Gibson-Ashby scaling law. Y^{bulk} was taken as 80 GPa for massive gold. (b) Absolute values of Y^{eff}, secant moduli from part (a) and storage moduli from dynamic mechanical analysis (DMA), each for specimens predeformed by $4-7\%$ plastic strain. Error bars represent sample-to-sample variance in several independent measurements. Results of studies of size-dependent Y^{eff} by thin-film buckling [33] and nanoindentation [32] are shown for comparison.

stages of compression (see Figure 6). The anomalously high compliance of NPG is not readily reconciled with available models for foams or network structures.

Figure 6(b) compares the observations from Figure 6(a) to independent measurements. Besides plotting the secant values of Y^{eff} at a given value of the plastic strain ($\varepsilon = 4-7\%$) versus L, the figure shows Y^{eff} at the same prestrain, measured as the storage modulus in a dynamic mechanical analyzer (DMA; for procedures see [34]). Both data sets agree well, both by magnitude and in respect to an unambiguous trend of 'smaller is stiffer'. The data comprises results from different batches, which all consistently support the observation.

In view of the significant stiffening at small size, as indicated by the present data, it is remarkable that results, included in Figure 6(b), of published studies on the size-dependent stiffness of NPG disagree widely. While an investigation by nanoindentation found no noticeable size dependence,[32] experiments using thin film buckling find a very pronounced increase of the stiffness with decreasing L.[33] It has also been pointed out [34] that thin film and indentation tests are sensitive to the regions

near the macroscopic sample surface, which may be denser than the bulk of NPG. Such experiments would then overestimate the stiffness, and the present data for bulk samples may be considered more accurate.

Experimental stiffness data is affected by residual silver, which brings the solid fraction above the estimated value, again resulting in an anomalously high stiffness of the porous metal.[32] Precise data for φ, for instance based on volume, mass and composition as in the present work, is mandatory but may not have been available in all published studies.

To summarize, tests on macroscopic samples of NPG show more stiffness at smaller size, implying that NPG should be anomalously stiff. Yet, the stiffness is indeed considerably less than predicted by continuum models for the elastic response of networks or foam. The origin of this discrepancy remains unclear and merits further studies. Aspects will now be highlighted.

7. Stiffening by surface excess elasticity, softening by shear instability? The observations on the elastic behavior of NPG are closely related to the issue of the effective elasticity of nano-objects such as nanowires. As has been briefly reviewed in [34], the available empirical data leave room for discussion whether small objects are stiffer, more compliant, or not modified at all compared to macroscopic parts. Molecular dynamics simulations appear inappropriate to the problem, and ab initio density functional theory allows for either, stiffening or softening at the surface depending on the crystallography.[40] The clear trend of more stiffness at small ligament size that emerges from the experiments on bulk NPG samples is therefore significant. As lesser size means more impact of the surface on the effective elastic behavior, the stiffening at small size strongly suggests that the surface regions are stiffer than bulk. In other words, the surface excess elastic modulus, on average over all surface orientations in NPG, appears to be positive-valued.

It is also significant that theory [41] as well as experiment [42] points toward nonlinear bulk elasticity as relevant for the effective elastic response of nanomaterials. Ngô et al. [25] have pointed out that the most obvious phenomenon in the latter context is the shear instability at the points of inflection of the generalized stacking-fault energy function. In fact, experiment [6] as well as numerical simulation [25,43] show that the surface-induced prestress in the bulk of the ligaments, which on theoretical grounds must have a large shear component,[44] is extremely high and can induce spontaneous plastic yielding even when there is no external load. It is thus conceivable that surface-induced shear stresses may bring some of the ligaments locally close to a shear-unstable state. Ngô et al. [25] suggests that these configurations may be responsible for the anomalously compliant behavior of NPG.

The observations on the effective elastic response of NPG appear contradictory, on the one hand a much higher compliance than expected for foams or network materials at the given φ-value, and on the other hand a trend for stiffening at smaller ligament size. It is thus not surprising that the above suggestions for the role of surface and nonlinear bulk elasticity embody opposing trends. Neither on their own nor in combination can they provide a natural explanation for all observation simultaneously. Further research into the fascinating elastic behavior of NPG appears of high interest.

8. Role of surface state As a result of their large specific surface area, the mechanical behavior of nanoporous metals must be sensitive to the environment and the surface chemistry. Exploring the impact of this sensitivity for the empirical database on small-scale plasticity and elasticity is one of the incentives for experiments in which NPG is converted into a hybrid material, in which the metal network and water or, more precisely, aqueous electrolyte, form the two constituent phases. This establishes two independent electric conduction pathways (electrons in the metal and ions in the solution) in the microstructure, separated capacitively by the electrochemical double layer. The superficial electric charge density and/or the adsorbate coverage on the pore surfaces can thus be controlled by applying an electric bias potential. In situ mechanical tests on these materials may unravel the impact of the surface state on various mechanical characteristics. The other incentive is that those hybrid materials actually exemplify a design strategy for novel functional nanomaterials, in which the macroscopic materials properties can be switched by tuning the state of the internal interfaces under control of an external potential.[45,46]

Among the studies that have successfully exploited the above material's design strategy by using NPG are the demonstration of large stroke actuation [9] and of switchable electric resistance.[47] The impact of the surface state on the issues of interest in the present context, namely strength [19] and stiffness,[34] will now be discussed in more detail.

In situ observations of the effective elastic response during potential cycles on NPG-based hybrid materials explore the impact of the local elastic behavior at the surface for the effective stiffness of NPG. This is illustrated by the pronounced and reproducible variation of Y^{eff}—as measured in a DMA—when the potential is modulated, see Figure 7(a).[34] It is well established that the electrode processes involve changes in the local charge density or adsorbate coverage exclusively at the surface. The observation of stiffness alternations by as much as 10% (Figure 7) therefore confirms a substantial contribution of the surface excess elasticity to the elastic

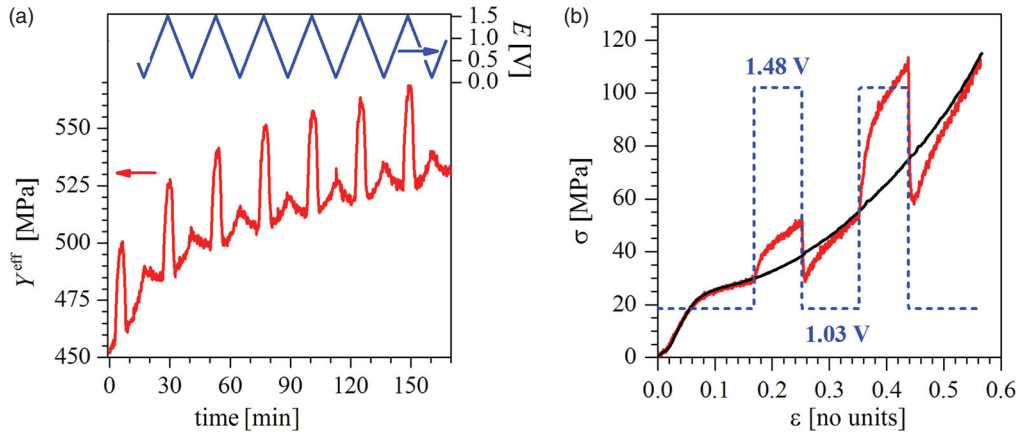

Figure 7. Effect of the surface state on mechanical properties of NPG. Results of in-situ testing with potential control in electrolyte. (a) The effective macroscopic Young's modulus Y^{eff}, as detected by dynamic mechanical analysis, varies during cycles of the electrode potential, E, versus the standard hydrogen electrode (after [34]; $L = 40$ nm). (b) During compression test the macroscopic flow stress, σ, varies as the surface state is switched between clean (potential 1.03V) and covered by one molecular monolayer of OH (1.48 V) (after [19]; $L = 20$ nm).

behavior of NPG. In fact, the modulation of the apparent excess thickness parameter τ of Section 4 takes on substantial amplitudes: 88 pm during purely capacitive charging and as much as 430 pm (equivalent to roughly two full atomic monolayers of gold!) when one monolayer of OH^--ions adsorbs.[34] These observations lend strong support to the conjecture of a significant contribution of the surface excess elasticity on the effective macroscopic elastic behavior of NPG, even in its dry state.

The impact of the surface state on the mechanical behavior of NPG is even more pronounced when it comes to strength. This was first demonstrated by Jin et al.,[19] who performed compression tests under potential control with a NPG-based hybrid material. As is exemplified in Figure 7(b), changes in the surface state allow the flow stress to be modulated by the remarkable factor of two. In the example of the figure, the variation accompanies the adsorption of one molecular monolayer of OH^- ions on the ligament surfaces. The observation indicates that the surface plays a vital role in controlling the flow stress and, thereby, the strength in nanoscale plasticity. The recent reports from the groups of Jin on electrochemically controlled creep rate [20] and of K. Sieradzki on the impact of adsorbate coverage on fracture toughness [24] of NPG further emphasize this finding. Modulating the surface behavior electrochemically therefore provides new opportunities, as yet to be exploited in depth, for exploring the mechanisms that govern small-scale mechanical behavior.

An implication of the above observations is that studies of small-scale plasticity can be severely affected by even small contaminations on surfaces; this implies that a precise characterization not only of topological features and relative density, but also state of the surface state is vital for achieving reproducible results. That type of characterization, with the required, sub-monolayer precision, was not typically available in published reports in the field.

9. Role of network connectivity? Our discussion of the empirical findings on strength and stiffness of NPG advertises a systematic trend for (somewhat) lesser strength and (considerably) lesser stiffness in the macroscopic samples of focus herein compared to other samples. Among the various aspects that may be connected to this discrepancy, the solid fraction stands out. While the present samples are made from $Ag_{75}Au_{25}$ master alloys, several other studies use master alloys of higher Au fraction, which results in higher φ. If the difference in strength and stiffness was simply due to different φ, then the observation would indicate a systematic deviation from the Gibson-Ashby laws. This could be understood if the geometry of the network were to depend on φ, possibly even approaching a discontinuous transition at a finite φ-value. The loss in percolation of load-bearing paths in the network would exemplify such a transition.

Support for a transition in the network structure comes from studies of spinodal decomposition. Several numerical simulation studies have used that process to create microstructures that closely resemble experimental NPG.[25,36,48] It is therefore remarkable that spinodal structures with unequal phase fractions are known to disintegrate during coarsening.[49,50] For NPG this implies that networks with low φ may exhibit a reduced connectivity density of their load-bearing paths, which would make them anomalously weak and compliant.

One may take the opposite point of view and emphasize the amazing success of the Gibson-Ashby scaling in describing the local strength of NPG in excellent agreement with the completely independent rule-of-mixture

analysis of NPG-based composite flow behavior, see Figure 4(b). Broken ligaments can be seen in experimental tomographic reconstructions and in the spinodal microstructures of the simulation studies, yet their low frequency argues against a strong impact on the mechanics. Furthermore, the stiffness increases drastically during the early stages of plastic compression of NPG, while the connectivity density is not expected to change significantly. Lastly, a direct comparison [25] between MD simulation and experiment on our samples shows excellent agreement in terms of strength as well as stiffness, even though the simulation uses an apparently perfectly connected network. Thus, the origin of the high compliance of macroscopic NPG samples must be qualified as simply not settled and in need of further experiments.

The question arises, how can one define and measure a suitable network connectivity parameter in experiment? In fact, three-dimensional tomographic reconstruction based on transmission electron microscopy [51,52] and X-ray [53] data has been demonstrated, and focused-ion-beam based serial sectioning [54] may provide even larger and statistically more representative reconstructions. Stereological analysis then supplies mean diameters of the ligaments (size L in this work) and pores (size L_P). A less obvious size parameter relates to the topological genus, g,[55] which is a measure for the number of closed rings (or 'handles') in a sample. These rings can be associated with load-bearing paths, and their characteristic mean size, L_R, relates to volume, V, per genus via $L_R \propto \sqrt[3]{V/g}$. Figure 8 illustrates the impact of R and of the L on the mechanical behavior. A 'well-connected' structure has, roughly, $L_R \sim L + L_P$. By contrast, a structure with many broken connections tends to have $L_R \gg L + L_P$, and part of its solid phase is not load-bearing. On top of the solid fraction, φ, we therefore propose to explore the connectivity parameter,

$$c_c = \frac{(L + L_P)}{L_R} = (L + L_P)\sqrt[3]{\frac{g}{V}} \qquad (6)$$

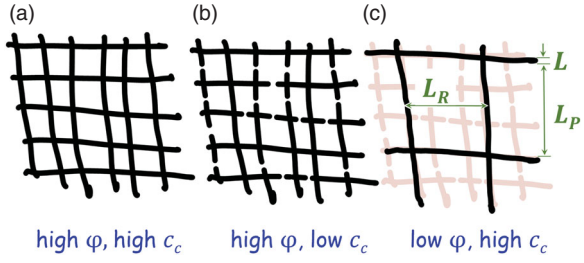

Figure 8. Networks with different solid fraction, φ, and connectivity, c_c. (a) and (b) have nearly identical ligament diameter, L, and pore diameter, L_P, and similarly high φ. Yet, broken ligaments make the characteristic diameter, L_R, of the load bearing ring in (b) much larger than in (a), implying lesser connectivity and more fragile mechanical behavior. (c) has the same load bearing ring as (b), suggesting similar mechanical behavior in spite of the very different φ.

as a supplementary measure for the mechanical sturdiness of networks. Specifically, if c_c of NPG were to decrease substantially at low solid fraction, then a systematic deviation from the Gibson-Ashby-type scaling equations—which presuppose constant connectivity density at all φ—would be expected for NPG.

10. Conclusions The present findings advertise the outstanding reproducibility obtained with macro-scale tests of NPG, specifically in regard to the trends for strength and stiffness versus ligament size. This confirms NPG as a highly significant model system for testing small-scale mechanical behavior.

The well-established trend of smaller is stronger is confirmed by the NPG data, yet with a numerically larger size-exponent than reported for other gold nanostructures and, remarkably, with a significantly lesser absolute value of the strength. Nonetheless, independent data from NPG-reinforced polymer nanocomposites confirm that the Gibson Ashby scaling relation applies quantitatively for NPG. This, along with the excellent agreement between molecular dynamics simulation of the flow behavior and experiment, argues against imperfections at the scale of the network structure as the reason for the lesser strength. One is lead to question whether previous data overestimates the impact of small scale alone on the strength.

The clear trend for substantially higher stiffness of NPG at smaller ligament size is significant in view of previous, contradictory reports on the size-dependent stiffness of nanoscale objects. Experiments with environmental control emphasize the contribution of the surface to the effective stiffness. Yet, similar to the strength, the stiffness of NPG is less (and quite significantly so in this instance) than predicted by simple geometrical models for foams or network structures. Conceivable origins include nonlinear elasticity in the bulk and specifically a shear instability at small size, or an anomalously reduced connectivity density in networks with small solid fraction.

Not all of the above propositions are mutually compatible, and the available evidence is inadequate for discriminating between them. Yet, each of these phenomena touches upon the fundamentals of materials behavior at small size and/or high porosity. Studying the mechanical behavior of macroscale NPG samples and its link to the microstructure is thus of high interest for future research.

Acknowledgments Some figures are reproduced with permission from Elsevier (Figures 1(b) and 7(a)) and AAAS (Figure 7(b)).

Disclosure statement No potential conflict of interest was reported by the authors.

Funding This work was supported by Deutsche Forschungsgemeinschaft through SFB 986 'Taylor-Made Multiscale Materials Systems - M^3', projects B2 and B4.

Note

1. Hardness H and effective macroscopic strength σ^{eff} of metal foams are related via $H \approx \sigma^{\text{eff}}$ (Tabor factor 1). Exploiting the opportunities of macroscopic tests on NPG, Jin et al. [7] have compared σ^{eff} to H in experiments on NPG. Their experiment indicates $H \approx 3\sigma^{\text{eff}}$ (Tabor factor 3), consistent with what is found for many massive materials. The finding underlines the distinction between dealloying-made nanoporous solids and metal foams, and it advertises the misconceptions that may arise if network structures such as NPG are inappropriately termed foams. The different mechanical behavior has been related to the differences—emerging from EBSD studies—in the deformation modes [7]: homogeneous strain in NPG versus the localized crush bands in foams.

References

[1] Louat NP, Duesbery MS, Imam MA, Provenzano V, Sadananda K. On dispersions of voids as sources of strength. Phil Mag Lett. 1991;63:159–163.
[2] Biener J, Hodge AM, Hayes JR, et al. Size effects on the mechanical behavior of nanoporous Au. Nano Lett. 2006;6:2379–2382.
[3] Volkert CA, Lilleodden ET. Size effects in the deformation of sub-micron Au columns. Phil Mag. 2006;86:5567–5579.
[4] Biener J, Hamza AV, Hodge AM. Deformation behavior of nanoporous metals. In: Yang F, Li JCM, editors. Micro and nano mechanical testing of materials and devices, chap. 6. New York, NY: Springer; 2008. p. 118–135.
[5] Weissmüller J, Newman RC, Jin HJ, Hodge AM, Kysar JW. Nanoporous metals by alloy corrosion: formation and mechanical properties. MRS Bulletin. 2009;34:577–586.
[6] Parida S, Kramer D, Volkert CA, Rösner H, Erlebacher J, Weissmüller J. Volume change during the formation of nanoporous gold by dealloying. Phys Rev Lett. 2006;97:035504.
[7] Jin H-J, Kurmanaeva L, Schmauch J, Rösner H, Ivanisenko Y, Weissmüller J. Deforming nanoporous metal: Role of lattice coherency. Acta Mater. 2009;57:2665–2672.
[8] Snyder J, Asanithi P, Dalton AB, Erlebacher J. Stabilized nanoporous metals by dealloying ternary alloy precursors. Adv Mater. 2008;20:4883–4886.
[9] Jin H-J, Wang X-L, Parida S, Wang K, Seo M, Weissmüller J. Nanoporous Au-Pt alloys as large strain electrochemical actuators. Nano Lett. 2010;10:187–194.
[10] Li R, Sieradzki K. Ductile-brittle transition in random porous Au. Phys Rev Lett. 1992;68:1168–1171.
[11] Wang K, Kobler A, Kübel C, Jelitto H, Schneider G, Weissmüller J. Nanoporous-gold-based composites: Toward tensile ductility. NPG Asia Mater. 2015;7:e187.
[12] Biener J, Hodge AM, Hamza AV, Hsiung LM, Satcher JH. Nanoporous Au: A high yield strength material. J Appl Phys. 2005;97:024301.
[13] Volkert CA, Lilleodden ET, Kramer D, Weissmüller J. Approaching the theoretical strength in nanoporous Au. Appl Phys Lett. 2006;89:061920.
[14] Zhu J, Seker E, Bart-Smith H, et al. Mitigation of tensile failure in released nanoporous metal microstructures via thermal treatment. Appl Phys Lett. 2006;89:133104.
[15] Lee D, Wei X, Chen X, et al. Microfabrication and mechanical properties of nanoporous gold at the nanoscale. Scripta Mater. 2007;56:437–440.
[16] Hodge AM, Biener J, Hayes JR, Bythrow PM, Volkert CA, Hamza AV. Scaling equation for yield strength of nanoporous open-cell foams. Acta Mater. 2007;55:1343–1349.
[17] Hakamada M, Mabuchi M. Mechanical strength of nanoporous gold fabricated by dealloying. Scripta Mater. 2007;56:1003–1006.
[18] Seker E, Gaskins JT, Bart-Smith H, et al. The effects of annealing prior to dealloying on the mechanical properties of nanoporous gold microbeams. Acta Mater. 2008;56:324–332.
[19] Jin H-J, Weissmüller J. A material with electrically tunable strength and flow stress. Science. 2011;332:1179–1182.
[20] Ye X-L, Jin H-J. Electrochemical control of creep in nanoporous gold. Appl Phys Lett. 2013;103:201912.
[21] Wang K, Weissmüller J. Composites of nanoporous gold and polymer. Adv Mater. 2013;25:1280–1284.
[22] Huber N, Viswanath RN, Mameka N, Markmann J, Weißmüller J. Scaling laws of nanoporous metals under uniaxial compression. Acta Mater. 2014;67:252–265.
[23] Briot NJ, Kennerknecht T, Eberl C, Balk TJ. Mechanical properties of bulk single crystalline nanoporous gold investigated by millimetre-scale tension and compression testing. Phil Mag. 2014;94:847–866.
[24] Sun S, Chen X, Badwe N, Sieradzki K. Potential-dependent dynamic fracture of nanoporous gold. Nat. Mater. 2015;14:894–898.
[25] Ngô B-ND, Stukowski A, Mameka N, Markmann J, Albe K, Weissmüller J. Anomalous compliance and early yielding of nanoporous gold. Acta Mater. 2015;93:144–155.
[26] Cattarin DSK, Lui A, Musiani MM. Preparation and characterization of gold nanostructures of controlled dimension by electrochemical techniques. J Phys Chem C. 2007;111:12643.
[27] Jin H-J, Parida S, Kramer D, Weissmüller J. Sign-inverted surface stress-charge response in nanoporous gold. Surf Sci. 2008;602:3588–3594.
[28] Rouya E, Cattarin S, Reed ML, Kelly RG, Zangari G. Electrochemical characterization of the surface area of nanoporous gold films. J Electrochem Soc. 2012;159:K97.
[29] Erlebacher J, Aziz M, Karma A, Dimitrov N, Sieradzki K. Evolution of nanoporosity in dealloying. Nature. 2001;410:450–453.
[30] Erlebacher J. An atomistic description of dealloying porosity evolution, the critical potential, and rate-limiting behavior. J Electrochem Soc. 2004;151:C614.
[31] Zhong Y, Markmann J, Jin H-J, Ivanisenko Y, Kurmanaeva L, Weissmüller J. Crack mitigation during dealloying of $Au_{25}Cu_{75}$. Adv Eng Mater. 2014;16:389–398.
[32] Hodge A, Doucette R, Biener M, Biener J, Cervantes O, Hamza A. Ag effects on the elastic modulus values of nanoporous Au foams. J Mater Res. 2009;24:1600–1606.
[33] Mathur A, Erlebacher J. Size dependence of effective Young's modulus of nanoporous gold. Appl Phys Lett. 2007;90:061910.
[34] Mameka N, Markmann J, Jin H-J, Weissmüller J. Electrical stiffness modulation—confirming the impact of

surface excess elasticity on the mechanics of nanomaterials. Acta Mater. 2014;76:272–280.
[35] Gibson LJ, Ashby MF. Cellular solids. 2nd ed. Oxford: Pergamon Press; 1999.
[36] Sun XY, Xu GK, Li X, Feng XQ, Gao H. Mechanical properties and scaling laws of nanoporous gold. J Appl Phys. 2013;113.
[37] Liu R, Antoniou A. A relationship between the geometrical structure of a nanoporous metal foam and its modulus. Acta Materialia. 2013;61:2390–2402.
[38] Jennings AT, Greer JR. Heterogeneous dislocation nucleation from surfaces and interfaces as governing plasticity mechanism in nanoscale metals. J Mater Res. 2011;26:2803–2814.
[39] Senior NA, Newman RC. Synthesis of tough nanoporous metals by controlled electrolytic dealloying. Nanotechnology. 2006;17:2311–2316.
[40] Zhou LG, Huang H. Are surfaces elastically softer or stiffer? Appl Phys Lett. 2004;84:1940.
[41] Liang H, Upmanyu M, Huang H. Size-dependent elasticity of nanowires: Nonlinear effects. Phys Rev B. 2005;71:241403.
[42] Chen LY, Richter G, Sullivan JP, Gianola DS. Lattice anharmonicity in defect-free pd nanowhiskers. Phys Rev Lett. 2012;109:125503.
[43] Farkas D, Crowson DA, Corcoran SG. Mechanical stability of nanoporous metals with small ligament sizes. Scripta Mater. 2009;61:497–499.
[44] Weissmüller J, Cahn JW. Mean stresses in microstructures due to interface stresses: a generalization of a capillary equation for solids. Acta Mater. 1997;45:1899–1906.
[45] Gleiter H, Weissmüller J, Wollersheim O, Würschum R. Nanocrystalline materials: A way to solids with tunable electronic structures and properties? Acta Mater. 2001;49:737–745.
[46] Weissmüller J, Viswanath RN, Kramer D, Zimmer P, Würschum R, Gleiter H. Charge-induced reversible strain in a metal. Science. 2003;300:312–315.
[47] Wahl P, Traussnig T, Landgraf S, Jin HJ, Weissmüller J, Würschum R. Adsorption-driven tuning of the electrical resistance of nanoporous gold. J Appl Phys. 2010; 108.
[48] Farkas D, Caro A, Bringa E, Crowson D. Mechanical response of nanoporous gold. Acta Mater. 2013;61:3249–3256.
[49] Lauger J, Lay R, Gronski W. The percolation-to-cluster transition during spinodal decomposition of an off-critical polymer mixture. Observation by light-scattering and optical microscopy. J Chem Phys. 1994;101: 7181.
[50] Lee JK, Han CD. Evolution of a dispersed morphology from a co-continuous morphology in immiscible polymer blends. Polymer. 1999;40:2521–2536.
[51] Rösner H, Parida S, Kramer D, Volkert CA, Weissmüller J. Reconstructing a nanoporous metal in three dimensions: An electron tomography study of dealloyed gold leaf. Adv Eng Mater. 2007;9:535–541.
[52] Fujita T, Qian LH, Inoke K, Erlebacher J, Chen MW. Three-dimensional morphology of nanoporous gold. Appl Phys Lett. 2008;92.
[53] Chen-Wiegart Y-cK, Wang S, Chu YS, et al. Structural evolution of nanoporous gold during thermal coarsening. Acta Mater. 2012;60:4972–4981.
[54] Uchic MD, Holzer L, Inkson BJ, Principe EL, Munroe P. Three-dimensional microstructural characterization using focused ion beam tomography. MRS Bulletin. 2007;32:408–416.
[55] Erlebacher J. Mechanism of coarsening and bubble formation in high-genus nanoporous metals. Phys Rev Lett. 2011;106:225504.